RND3 IS ESSENTIAL FOR MITOCHONDRIAL INTEGRITY AND FUNCTION IN CARDIOMYOCYTES

A Thesis

by

KELSEY COLLEEN ANDRADE

Submitted to the Office of Graduate and Professional Studies of
Texas A&M University
In partial fulfillment of the requirements for the degree of

MASTER OF SCIENCE

Chair of Committee,	Jiang Chang
Committee Members,	Keigi Fujiwara
	Yu Liu
Head of Program,	Warren Zimmer

May 2018

Major Subject: Medical Sciences

ABSTRACT

Small GTPase Rnd3 participates in a broad spectrum of pathological processes. The downregulation of Rnd3 is observed in heart failure patients, and causes cardiac dysfunction in animal models. The dysfunction of mitochondria is one of the key factors contributing to heart failure. Whether Rnd3 downregulation plays a regulatory role in mitochondrial dysfunction in the heart remains unknown. Using genetic Rnd3 haploinsufficient mice, we demonstrated for the first time to our knowledge, that the decreased expression of Rnd3 causes mitochondrial dysfunction, which results in reduced ATP production and increased generation of reactive oxygen species (ROS), and eventually cell apoptosis. We revealed the associated molecular mechanism, in which Rnd3 deficiency leads to intracellular calcium overload, and consequently increased mitochondrial calcium levels. The latter triggers mitochondrial dysfunction. Calcium uptake inhibitor Ru360 treatment partially rescues this cellular phenotype. We conclude that a normal expression level of Rnd3 is essential for mitochondrial integrity and function in the heart.

I would like to dedicate this thesis in loving memory of Pennie and Christo,

and to all my family and friends for their love and support.

ACKNOWLEDGMENTS

I would like to express my gratitude to my former lab members and dear friends, Xiaojing Yue and Xiangsheng Yang, who contributed a lot of hard work and time to this scientific research project as well as provided me with guidance and friendship. Additionally, I am grateful for the contributions from Xi Lin, Yanhong Yu, Yuan Dai, Xin Yi, Dale J Hamilton, Anisha A Gupte, Aijun Zhang, Tingli Yang, Junli Guo, Qi Li, and Yanlin Ma. I would like to thank my committee members, Keigi Fujiwara, Yu Liu, and especially my PI, JC, for the mentorship and support. Lastly, I would like to especially thank my fiancé, Reid T Powell, for his constant love and support.

CONTRIBUTORS AND FUNDING SOURCES

Contributors

The following work was supervised by a thesis committee consisting of Jiang Chang of the Center of Translational Cancer Research at Texas A&M University, Keigi Fujiwara of the Department of Cardiology at University of Texas MD Anderson Cancer Center, and Yu Liu of the Department of Biology and Biochemistry at University of Houston.

I thank the Institutional Core Grant CA16672, High Resolution Electron Microscopy Facility, University of Texas MD Anderson Cancer Center for providing the electron microscopy service. I am also grateful to Xiangsheng Yang and Xiaojing Yue for their collaboration and technical support for these data.

Funding Sources

This work was supported by the National Natural Science Foundation of China 81601317, the Chinese Postdoctoral Fellowship 2015M580726 (X. Yue); the AHA Postdoctoral Fellowship 13POST17260043 (X. Yang); the State Key Development Program for Basic Research of China 2012CB966502, National Natural Science Foundation of China 81270716 and 81471464 (Y. Yu); National Natural Scientific Foundation of China 81460042 and 81160020 (J. G.); the American Heart Association Grant-in-Aid 20500033, the National Institutes of Health NIH-NHLBI R01HL102314 and the NIH-NHLBI R01HL123953 (J.C.).

TABLE OF CONTENTS

LIST OF FIGURES

NOMENCLATURE

ROS - reactive oxygen species

ROCK1 - Rho-associated coiled-coil protein kinase 1

TAC - transverse aortic constriction

RyR2 - ryanodine receptor 2

NAD - nicotinamide adenine dinucleotide

β2AR - beta-2 adrenergic receptor

PKA - protein kinase A

MOMP - mitochondrial outer membrane permeability

VDACs - voltage-dependent anion channels

MCU - mitochondrial calcium uniporter

DHE - dihydroethidium

SR - sarcoplasmic reticulum

1. INTRODUCTION

Rnd3 is a constitutively active small Rho GTPase and a repressor of Rho-associated coiled-coil protein kinase 1 (ROCK1) [1-3]. Rnd3 is ubiquitously expressed in most tissues, including the heart [4-6]. Emerging evidence indicates a broad spectrum of functions of Rnd3 that might be independent of RhoA/ROCK1 signaling [7-11]. We first discovered that Rnd3 protein levels were significantly downregulated in heart failure patient myocardia [8, 12]. The downregulation of Rnd3 has also been linked to various types of cancer [13-16]. To explore the pathological significance of Rnd3 downregulation, we used a genetic approach and demonstrated that Rnd3 heterozygous ($Rnd3^{+/-}$) mice were predisposed to hemodynamic stress which resulted in apoptotic cardiomyopathy and heart failure after pressure overload [8]. Furthermore, we found that Rnd3 deficiency impaired calcium homeostasis in both cardiomyocytes and non-cardiomyocyte cells. Complete loss of Rnd3 was embryonically lethal; the mutant mice developed several cardiac arrhythmia phenotypes and died at E11.5 due to calcium leakage from the sarcoplasmic reticulum (SR) [9]. However, the cellular phenotype and the consequences of the calcium leakage induced by Rnd3 deficiency have not been defined.

Cytosolic calcium overload has numerous detrimental cellular effects and is linked to many pathological conditions including cardiomyopathies [17]. The excessive increase of intracellular calcium in cardiomyocytes can alter many molecular signaling pathways and can also cause impairment of mitochondrial function; regulation of these systems is important for cellular homeostasis and survival. Mitochondrial dysfunction is one of the major pathological consequences of calcium overload in cardiomyocytes and tightly coincides with cardiac remodeling and cardiovascular disease [18-20].

In continuation of our previous studies in which Rnd3 deficiency resulted in SR calcium leakage, we wanted to investigate the involvement of mitochondria in this Rnd3-deficiency mediated calcium overload cardiomyopathy. In this study, we used $Rnd3^{+/-}$ mice that underwent transverse aortic constriction (TAC) surgery to induce pressure overload and isolated $Rnd3^{+/-}$ cardiomyocytes as our *in vivo* and *in vitro* models, respectively. Isolated mitochondria from these $Rnd3^{+/-}$ models displayed impaired function when measured using the Seahorse Bioscience XF Analyzer, as well as hyperpolarized membrane potentials with excessive reactive oxygen species (ROS) generation. Our data expound our previous demonstration of the involvement of Rnd3 in the tight regulation of intracellular calcium and calcium-dependent signaling pathways and form the connection of mitochondrial stress to increased cardiomyocyte apoptosis.

In this study, we identify the cellular phenotype of cardiomyocytes that results from Rnd3 deficiency and add to the complexity of the molecular mechanism involved in calcium overload-induced mitochondrial damage, which is often observed in heart failure, as well as expand the knowledge of the biological functions of Rnd3 and its function in the heart.

2. MATERIALS AND METHODS

Generation and verification of Rnd3 haploinsufficient mouse line and transverse aortic constriction (TAC) surgery

The establishment of the Rnd3 haploinsufficient mouse line was previously described [21]. Genomic DNA was extracted from the tails for the purpose of genotyping. TAC was conducted in 10-15 week-old adult male mice for 3 weeks as previously described, followed by cardiac function analysis [8]. All animal experiments were approved by the Institutional Animal Care and Use Committee of the Texas A&M University Health Science Center-Houston.

Electron microscopy analysis

Freshly harvested mouse cardiac left ventricles were fixed with a buffer containing 3% glutaraldehyde plus 2% paraformaldehyde in 0.1 M cacodylate buffer, pH 7.3, and then were processed and embedded in LX-112 medium. The ultrathin sections stained with uranyl acetate and lead citrate were examined in a JEM 1010 transmission electron microscope (JEOL, USA, Inc., Peabody, MA). Images were obtained with AMT Imaging System (Advanced Microscopy Techniques Corp, Danvers, MA).

Cardiomyocyte isolation, cell culture, hypoxic conditioning, and Ru360 treatment

The isolation of adult mouse cardiomyocytes was previously described [12]. Briefly, the fresh hearts were harvested from 10-15 week-old male mice with or without TAC stress. The mouse cardiomyocytes were isolated by enzymatic digestion with the Langendorff perfusion system (120108, Radnoti, CA, USA) followed by calcium reintroduction. The cells were cultured in laminin precoated dishes with 5% fetal bovine serum (FBS). Hypoxic conditions were obtained using a hypoxia chamber (MIC-101, Billups-Rothenberg Inc, CA, USA) with 1% O_2 for 16 h. For

Ru360 treatment, Ru360 (557440, EMD Millipore, Germany) was diluted in the culture medium with a final concentration of 5 μM.

Fluorescence staining

For histological analysis, whole hearts were embedded in Tissue-Tek O.C.T. Compound (4583, Sakura), and frozen sections were used for dihydroethidium (DHE) staining (D1168, Thermo Fisher Scientific, NY, USA). Pictures from each group (20) were taken under the 40x microscope objective. Images were analyzed by Leica Application Suite Imaging Software (Version 4.0, Germany).

Live mouse cardiomyocytes were used for Rhod-3 (R10145, Invitrogen, NY, USA), JC-1 (M34152, Thermo Fisher Scientific, NY, USA), and MitoSOX (M36008, Thermo Fisher Scientific, NY, USA) staining. TUNEL staining (11684795910, Roche, Penzberg, Germany) in fixed cells was performed for apoptosis detection. Images were acquired by Macro Confocal Imaging System (AZ-C2^{+}, Nikon, NY, USA). A total of 20 staining pictures from each group were quantified by NIS-Elements Advanced Research software (Nikon, NY, USA).

Assessment of mitochondrial function

Mitochondria were isolated from myocardial tissues of 10-15 week-old adult male mice from the sham or TAC surgery experimental groups as previously described [22]. Briefly, freshly isolated heart tissue was homogenized in isolation buffer (220 mM mannitol, 70 mM sucrose, 5 mM MOPS, 2 mM EGTA, 0.2% fatty acid-free BSA) on ice, followed by centrifugation at 800 rpm for 10 min. The pellet was removed and the supernatant was centrifuged at 12000 rpm for 10 min. The mitochondria were collected in the new pellet, and were purified by a series of centrifugation processes at 4℃. Mitochondria were finally suspended in a buffer that consisted

of 220 mM mannitol, 70 mM sucrose, 5 mM MOPS, and 0.5 mM EGTA. The concentration of the mitochondria was measured by Pierce BCA Protein Assay Kit (23225, Thermo Fisher Scientific, NY, USA).

Mitochondrial respiration was measured at 37℃ in XF24 Extracellular Flux Analyzer (Seahorse Bioscience, MA, USA). XF24 FluxPak (100867-100, Seahorse Bioscience, MA, USA) was used to determine mitochondrial oxygen consumption rates (OCR) in freshly isolated mitochondria. The mitochondrial assay solution (MAS) consisted of 70 mM sucrose, 220 mM mannitol, 5 mM KH_2PO_4, 5 mM $MgCl_2$, 2 mM HEPES, 1 mM EGTA, and 0.2% fatty acid-free BSA, pH 7.4. To measure complex I activity, mitochondria were supplied with MAS containing substrates of 5 mM pyruvate and malate. The OCRs were measured by subsequently adding 250 μM ADP, 2 μM oligomycin, 2 μM FCCP, and 4 μM antimycin A.

ATP synthesis measurement

A concentration of 0.3 μg of mitochondria supplied with 250 μM ADP, 5 mM pyruvate, and 5 mM malate was incubated at 37℃ for 6 min. The reaction was immediately terminated by adding 4 μM antimycin A. The ATP concentration was measured using ATP Assay System Bioluminescence Detection Kit (FF2000, Promega, Madison, USA).

Statistical analysis

Data were expressed as means ± S.D. Student's t-test was used for two-group comparison and one-way ANOVA (analysis of variance) was applied for a multiple group comparison. Welch's t-test was applied for the comparison of two groups with unequal sample sizes and non-parametric ANOVA was applied for multiple comparison groups of sample populations that do not fall in normal distribution. Statistical comparisons were performed using SigmaStat (Systat

Software Inc., San Jose, CA).

3. RESULTS

Rnd3 deficiency increased cardiomyocyte cytosolic calcium after TAC surgery

It is well known that calcium overload in cardiomyocytes results in dysfunction and cell death. Therefore, we first compared the overall calcium levels of $Rnd3^{-/+}$ and wild-type (WT) cardiomyocytes to confirm the Rnd3 deficiency-mediated calcium overload phenotype, resulting from SR leakage, after TAC. Briefly, cardiomyocytes were isolated from WT and $Rnd3^{+/-}$ mice either after undergoing TAC surgery or as part of a sham control group, and the cytosolic calcium concentrations were subsequently measured in both groups of the cultured cardiomyocytes. Rhod-3 staining was used to visualize the calcium in live cells and the fluorescence intensities were used for quantification. Significantly elevated calcium levels were observed in the cytosol of $Rnd3^{+/-}$ cardiomyocytes compared to the WT control in the sham group, and an even more pronounced elevation of calcium was detected in the $Rnd3^{+/-}$ cardiomyocytes after TAC-induced stress (Figure 1).

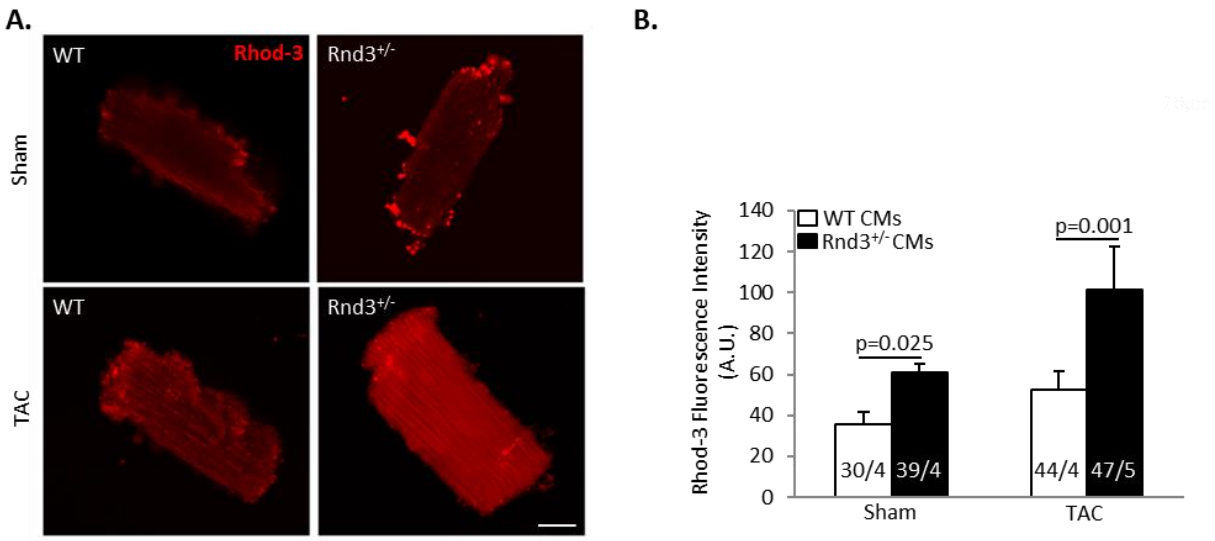

Figure 1. Calcium overload was detected in Rnd3$^{+/-}$ cardiomyocytes. A. An increase in the amount of calcium was detected in isolated Rnd3$^{+/-}$ cardiomyocytes, this increase was profoundly enhanced after TAC stress. Calcium was visualized by live cell Rhod-3 staining (red). Scale bar represents 20 µm. **B.** Cytosolic calcium was quantified by fluorescence intensity. The numbers in the columns represent the number of cardiomyocytes over the number of mice in each group. CMs: cardiomyocytes; TAC: transverse aortic constriction.

Myocardial mitochondria dysfunction occurred in Rnd3 haploinsufficient mice and was worsened in response to TAC stress

The influx in Rnd3$^{+/-}$ cardiomyocyte cytosolic calcium led us to examine the integrity of the mitochondria present in the myocardium after hemodynamic stress because the mitochondrion is a calcium sensitive organelle that is essential for cell function and survival. Electron microscopy of Rnd3$^{+/-}$ myocardium after TAC revealed damaged mitochondria along with disrupted myofibril structure and arrangement compared to the WT myocardium. The

compromised mitochondria displayed loss of cristae superstructure when viewed at a higher magnification (Figure 2A).

To further investigate the phenotype of the Rnd3 haploinsufficient mitochondria, functional analysis of the organelles was conducted by examining the basal mitochondrial respiratory control ratios as an indicator of the tightness of coupling between mitochondrial oxygen consumption and ATP production. Briefly, $Rnd3^{+/-}$ and WT mitochondria from both the TAC and sham group myocardial tissues were freshly isolated in medium containing succinate and phosphate substrate; these early conditions were referred to as State 2 for measurement purposes. ADP was then added which caused a sudden burst of oxygen uptake as the ADP was converted to ATP; this was State 3. The oxygen consumption and ATP synthesis rates for each state were measured using the Seahorse Bioscience XF analyzer and used to calculate the respiratory control ratios (State 3/State 2). $Rnd3^{+/-}$ mitochondria had substantially decreased basal respiratory control ratios in both the sham and even more so in the TAC experimental groups compared to the WT control groups (Figure 2B).

Next, we measured coupled oxygen consumption by the introduction of an ATP synthase inhibitor, Oligomycin; the chemical blocks the proton channel of ATP synthase and consequently disrupts oxidative phosphorylation. The decrease in the oxygen consumption is indicative of the coupled oxygen devoted to ATP synthesis. We found that the $Rnd3^{+/-}$ mitochondria displayed decreased coupled oxygen consumption compared to the WT under sham conditions (Figure 2C). A further decrease in the oxygen consumption was observed after TAC stress (Figure 2C).

The decrease in coupled respiration of the Rnd3$^{+/-}$ mitochondria led us to examine ATP synthesis driven by mitochondrial complex I. Nicotinamide adenine dinucleotide (NAD^+) is used as an electron acceptor for mitochondrial complex I during oxidative respiration and is a well-known source of ROS generation depending on the NAD^+/NADH ratio present in the mitochondrion. Additionally, complex I driven ATP synthesis was examined to ensure that the detected impairment in oxidative phosphorylation of the heterozygous mitochondria was not due to a complex-specific abnormality or alteration in the oxidative phosphorylation pathway, because complex II/Q electron transportation can work independently of complex I depending on the available substrates. Measurements were taken in the presence of complex I substrate, pyruvate/malate, and complex I inhibitor, rotenone, and then the measurements were compared to the basal respiratory control indexes to represent complex I driven ATP synthesis. Rnd3$^{+/-}$ mitochondria revealed impairment of mitochondrial complex I driven ATP synthesis compared to the WT control, suggesting impaired mitochondrial function in Rnd3$^{+/-}$ heart tissues due to the elevated calcium levels (Figure 2D).

Rnd3$^{+/-}$ mitochondria exhibited hyperpolarized membrane potentials after TAC

We then postulated that the elevated calcium influx and disrupted coupled respiration of the Rnd3$^{+/-}$ mitochondria would affect the mitochondrial membrane potentials. Therefore, we examined the membrane potentials of the mitochondria using JC-1 dye, a membrane potential sensitive dye. A shift from green to red fluorescence emission indicates an increased membrane potential. The ratio of red/green fluorescence showed no significant difference between the WT and Rnd3$^{+/-}$ cardiomyocytes under normal conditions. However, we detected a profound increase in the red/green fluorescence emission ratio in Rnd3$^{+/-}$ cardiomyocytes compared to

the WT control after TAC challenge (Figure 2E-F), suggesting hyperpolarized mitochondrial membrane potentials due to accumulation of calcium within the mitochondrial intermembrane space, which further interrupted mitochondrial essential functions, such as ATP synthesis; and could potentially result in excessive ROS generation.

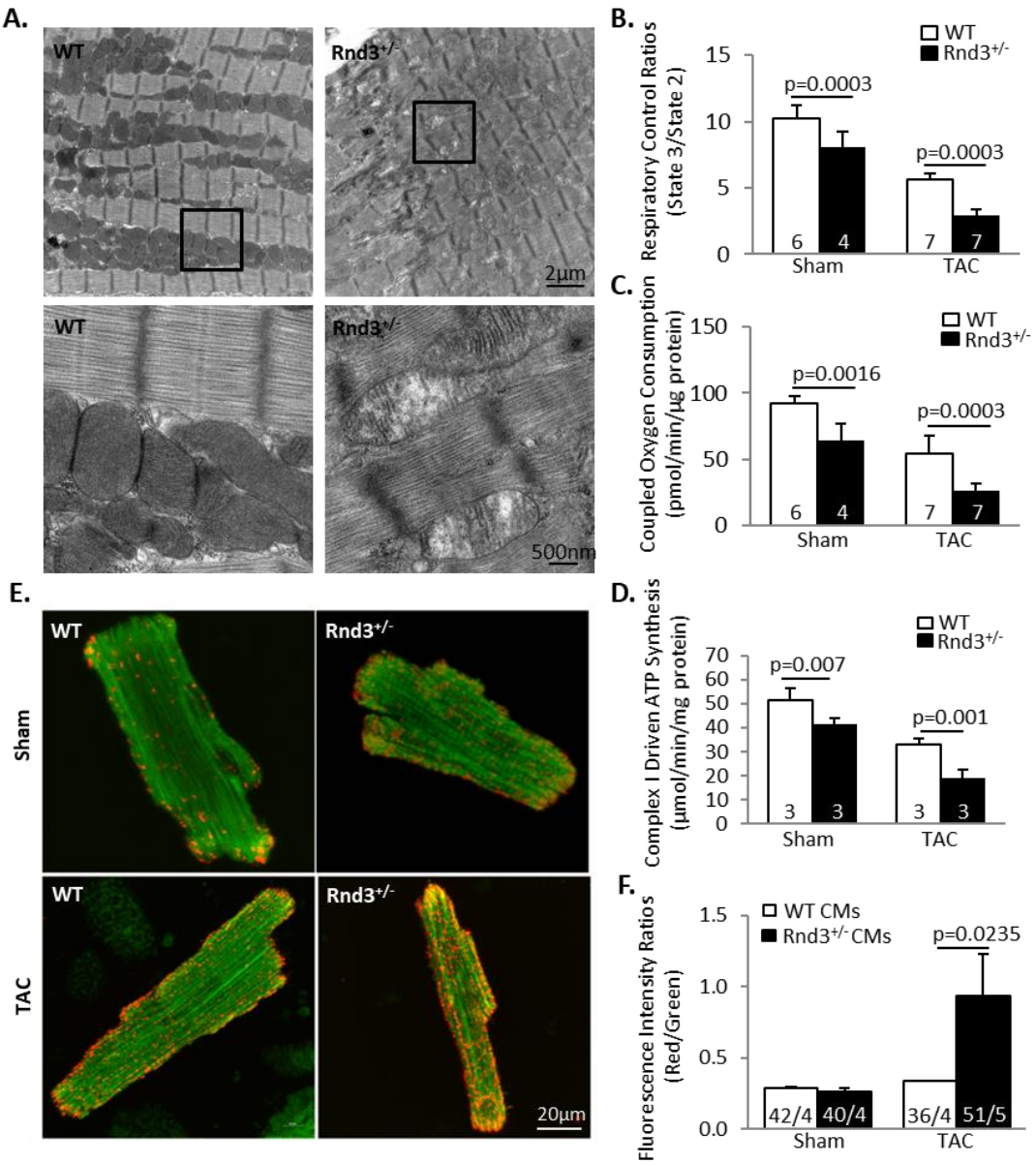

Figure 2. Rnd3$^{+/-}$ cardiomyocytes exhibited mitochondrial dysfunction. A. Electron microscopy showed mitochondrial damage in the Rnd3$^{+/-}$ myocardium compared to WT after TAC . Images of higher magnification displayed mitochondria losing cristae superstructure. **B.** Oxygen consumption rates (OCR) of freshly isolated WT and Rnd3$^{+/-}$ cardiac mitochondria from control sham and TAC groups were measured in the presence of succinate (State 2) and after injection of ADP (State 3). State 3/State 2 measurements were used as basal respiratory control ratios for mitochondria of each experimental group. Rnd3 deficiency resulted in impaired mitochondrial respiratory function. **C.** Rnd3$^{+/-}$ mitochondria displayed decreased coupled oxygen consumption respiratory rates compared to WT in both the sham and TAC groups. **D.** Complex I driven ATP synthesis was measured in WT and Rnd3$^{+/-}$ cardiac mitochondria in the presence of complex I substrate pyruvate/malate, with the addition of ADP and the complex I inhibitor rotenone, successively. A significant decrease in ATP synthesis indicated mitochondrial dysfunction in the Rnd3$^{+/-}$ myocardium after TAC. **E.** Hyperpolarized mitochondrial membrane potentials were detected in isolated Rnd3$^{+/-}$ cardiomyocytes compared to the WT control after TAC. The increase in mitochondrial membrane potentials was visualized by red fluorescence. **F.** Mitochondrial membrane potentials were quantified by the ratios of red/green fluorescence intensities for each experimental group. The numbers in the columns represent the number of cardiomyocytes over mice in each group. CMs: cardiomyocytes; TAC: transverse aortic constriction.

Elevated levels of ROS were detected in the Rnd3$^{+/-}$ myocardial tissues

Therefore, our previous findings led us to examine the overall mitochondrial ROS (superoxide) production levels in Rnd3$^{+/-}$ and WT mouse heart tissues with and without TAC surgery as the last definitive factor for the Rnd3-deficiency cellular phenotype. The superoxide indicator, dihydroethidium, was used to visualize ROS levels in frozen myocardial tissue sections. Red fluorescence occurs when the dye is oxidized and transported to the nucleus where it intercalates with the cellular DNA. The areas of the detected ROS from the Rnd3$^{+/-}$ and WT cardiac sections were quantified using LAS 4.0 software.

Substantially elevated ROS levels were observed in the Rnd3$^{+/-}$ myocardial tissues from both experimental groups compared to the WT controls. The Rnd3$^{+/-}$ tissue from the sham group displayed a higher ROS level compared to the WT control and this difference in the ROS levels was further increased after TAC stress (Figure 3).

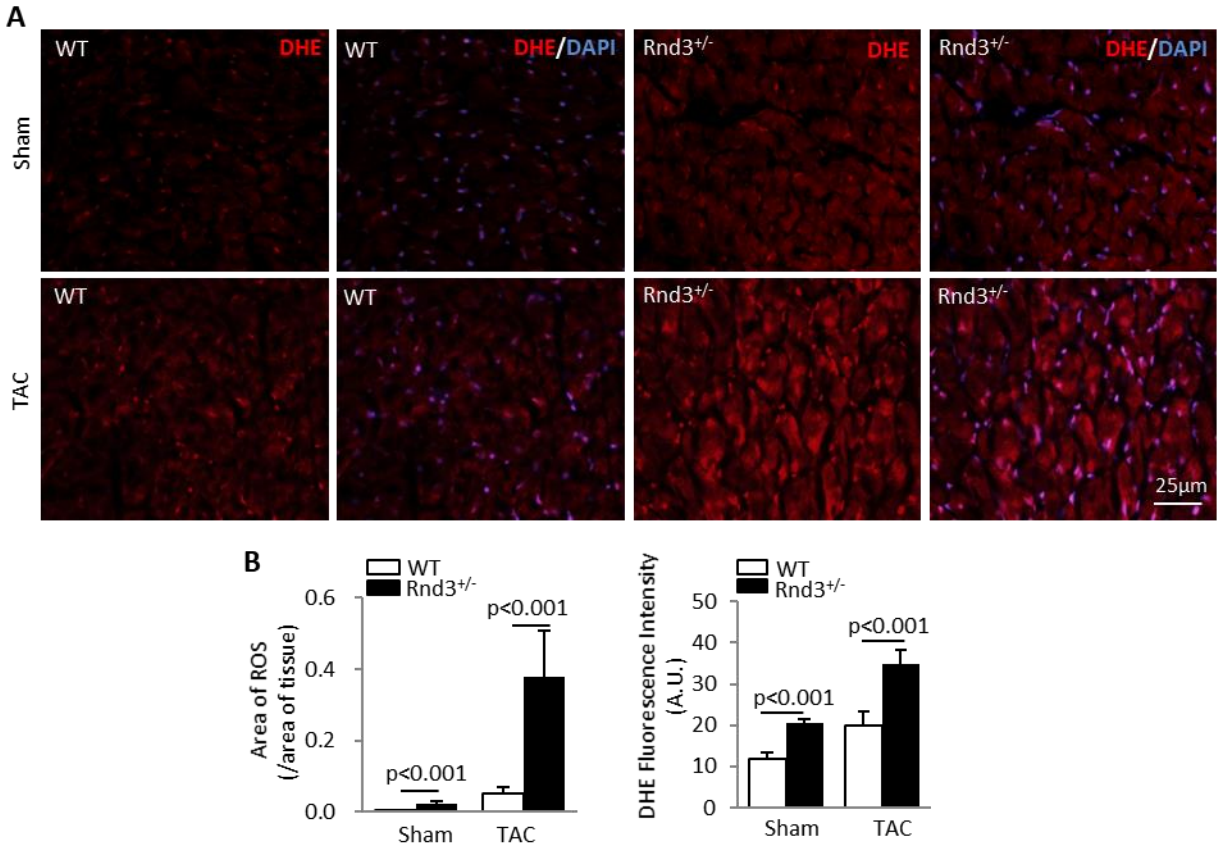

Figure 3. A significant increase in ROS generation was detected in the Rnd3$^{+/-}$ myocardium. A. Representative images of ROS in WT and Rnd3$^{+/-}$ myocardial tissues with or without TAC surgery. Dihydroethidium (DHE) staining for ROS was visualized by red fluorescence and DAPI counterstaining was shown in blue. **B.** ROS in cardiac sections was quantified by area and fluorescence intensity using LAS 4.0 software. Significant amounts of ROS were observed in the post-TAC Rnd3$^{+/-}$ myocardium. Data represent the average of 5 mice for each group. ROS: reactive oxygen species; TAC: transverse aortic constriction.

Mitochondria-specific calcium uptake inhibitor Ru360 partially rescued the mitochondrial dysfunction in Rnd3$^{+/-}$ cardiomyocytes after hypoxia

In an attempt to improve the Rnd3-deficiency cellular phenotype, we conducted a series of rescue experiments using Ru360, a mitochondrial calcium uptake inhibitor. Improved mitochondrial function was seen after Ru360 treatment. Briefly, Rnd3$^{+/-}$ and WT cardiomyocytes were isolated and exposed to hypoxic conditions for 16h to mimic *in vivo*

hemodynamic stress; the Rnd3$^{+/-}$ mitochondria isolated from the Ru360 treatment group exhibited a partially rescued basal respiratory control ratio, coupled oxygen consumption rate, and complex I driven ATP synthesis (Figure 4). The hyperpolarization of the mitochondrial membrane potential observed in the mitochondria isolated from Rnd3$^{+/-}$ cardiomyocytes after hypoxia exposure was also partially corrected after Ru360 treatment (Figure 5).

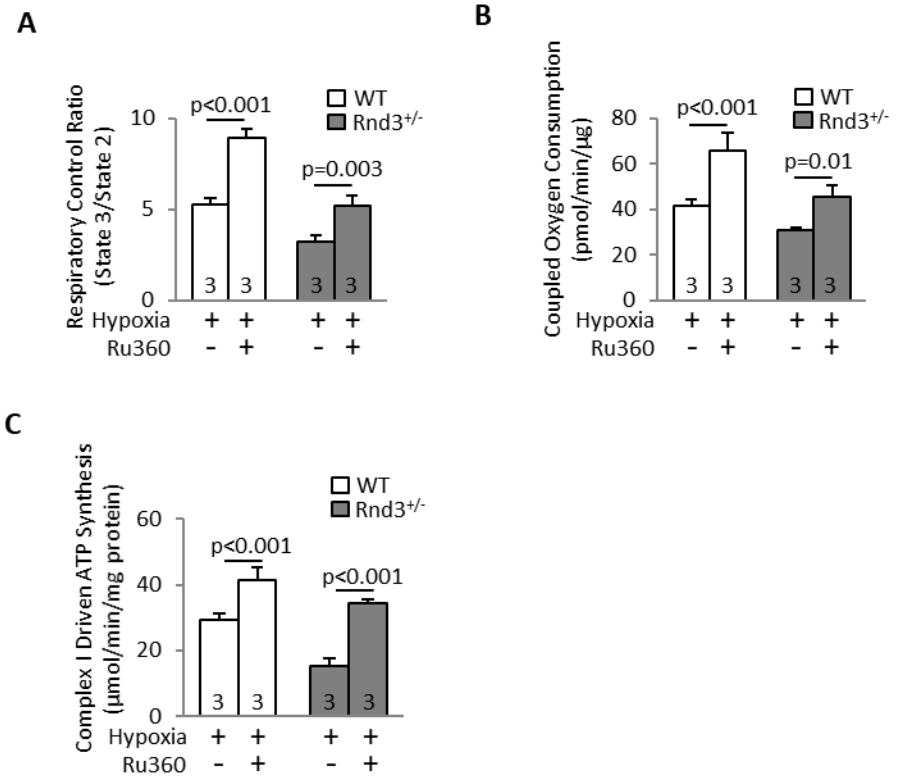

Figure. 4. Mitochondrial dysfunction in Rnd3$^{+/-}$ cardiomyocytes was partially rescued by mitochondria-specific calcium uptake inhibitor Ru360. Mitochondria were isolated from WT and Rnd3$^{+/-}$ cardiomyocytes after exposure to hypoxic conditions, and either with or without Ru360 treatment. The Rnd3 deficiency-mediated mitochondrial respiration impairment was improved after inhibition of mitochondrial calcium uptake; determined by measurements of the **A:** respiratory control ratios for State 3/State 2 **B:** the coupled oxygen consumption rates and **C:** complex I driven ATP synthesis. The numbers in the columns represent the number of mice used for cardiomyocyte isolation in each group.

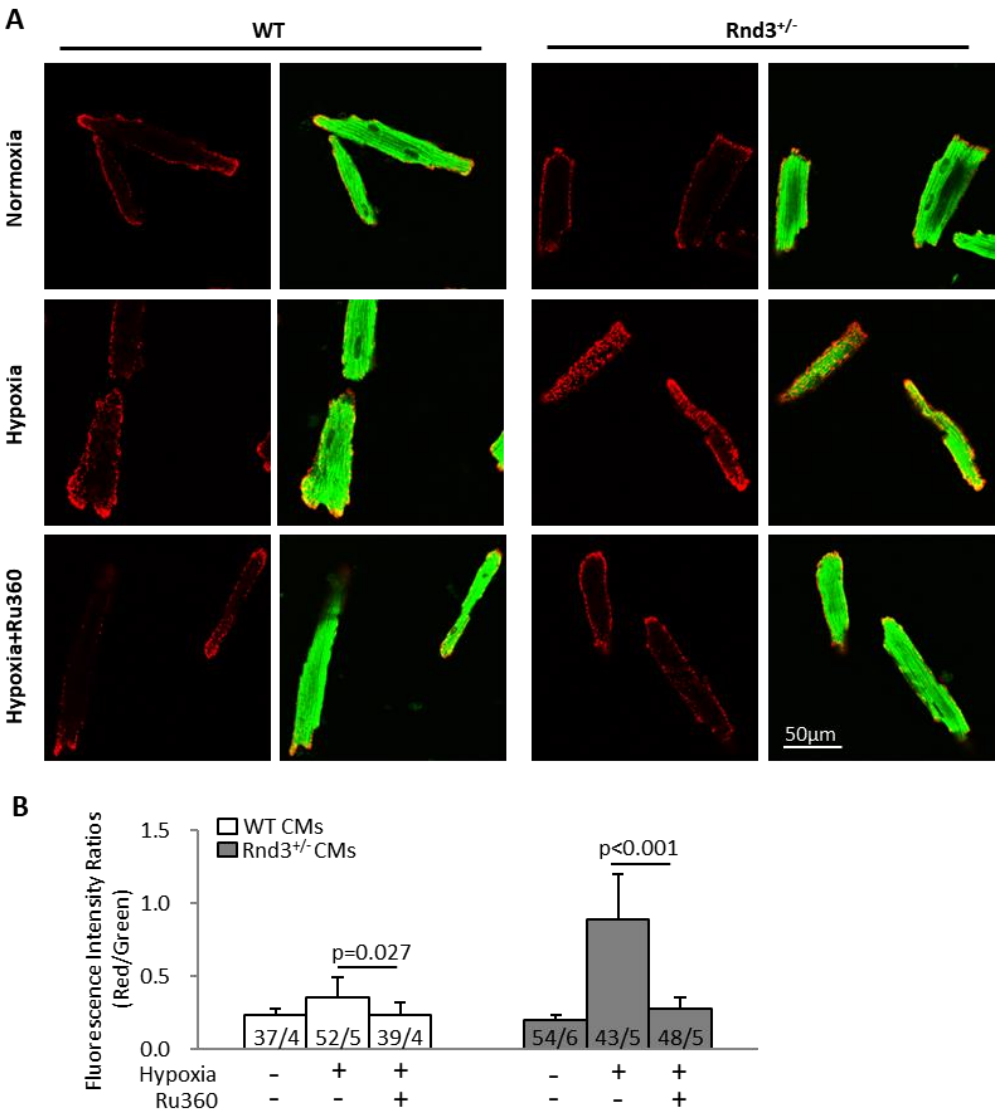

Figure 5. Ru360 partially rescued the Rnd3 deficiency-mediated hyperpolarization of mitochondrial membrane potentials in cardiomyocytes. A. Calcium uptake inhibitor Ru360 significantly attenuated the increased mitochondrial membrane potentials in Rnd3$^{+/-}$ cardiomyocytes. **B.** Mitochondrial membrane potentials were quantified by the ratio of red/green fluorescence intensities. The numbers in the columns represent the number of cardiomyocytes over the number of mice in each group. CMs: cardiomyocytes.

Finally, we assessed the mitochondrial ROS production using the MitoSOX assay after Ru360 treatment. We found that Ru360 treatment reduced the excessive ROS generation induced by hypoxia in the Rnd3$^{+/-}$ cardiomyocytes (Figure 6A-B). These data led us to conduct TUNEL staining in order to determine if there was an increase in the number of apoptotic Rnd3$^{+/-}$ cardiomyocytes under hypoxic conditions compared to the WT control, and if Ru360 treatment could also prevent the cells from undergoing apoptosis. As expected, there were significantly more TUNEL positive Rnd3$^{+/-}$ cardiomyocytes after hypoxic stress compared to the WT control. Furthermore, Ru360 treatment significantly decreased the Rnd3 deficiency-mediated apoptosis, as expected (Figure 6C-D).

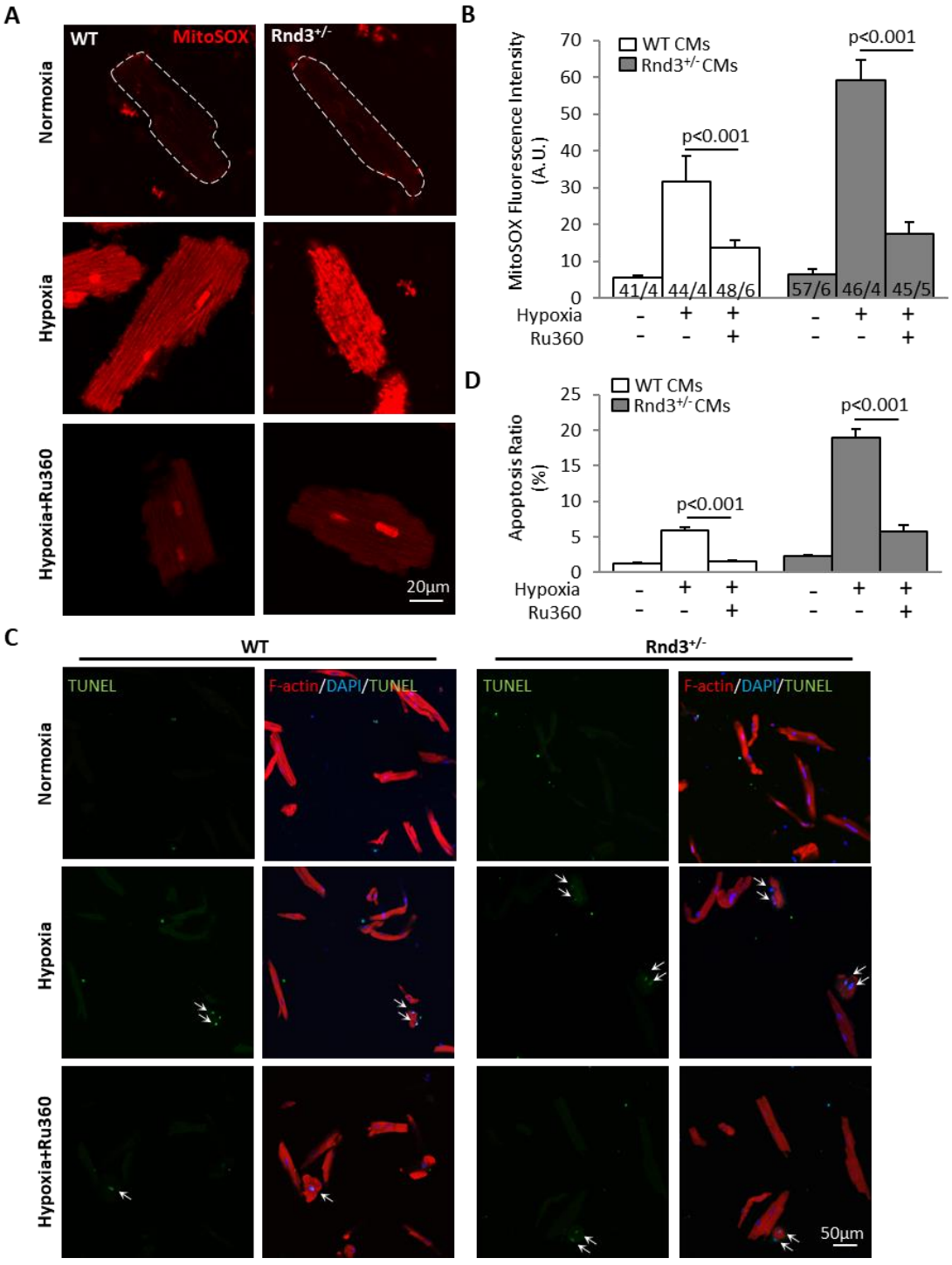

Figure 6. Ru360 attenuated ROS overproduction and apoptosis in Rnd3$^{+/-}$ cardiomyocytes. A. Excessive generation of ROS in Rnd3$^{+/-}$ cardiomyocytes was partially attenuated by Ru360 treatment. **B.** ROS was quantified by fluorescence intensity. **C.** Induced by hypoxic stress, a significant increase in TUNEL positive cells was observed in Rnd3$^{+/-}$ cardiomyocytes compared to the WT control. Ru360 administration partially rescued the Rnd3 deficiency-mediated cardiomyocyte apoptosis. The arrows indicate TUNEL positive cells (green) merged with DAPI nucleus counter-staining (blue). **D.** Quantification of the TUNEL positive cells. The numbers in the columns represent the number of cardiomyocytes over the number of mice in each group. CMs: cardiomyocytes.

Rnd3 is essential for mitochondrial function in cardiomyocytes

In summary, our previous study demonstrated that Rnd3 deficiency results in attenuation of β_2AR (Beta-2 adrenergic receptor) ubiquitination and lysosomal targeting, which leads to hyperactivation of protein kinase A (PKA) signaling. The excessive activation of PKA leads to hyperphosphorylation of ryanodine receptor 2 (RyR2) calcium release channels and causes RyR2 destabilization. The later results in calcium leakage from the SR, which causes cardiac arrhythmia [9]. Here, we have expanded the previous study and further defined the cardiomyocyte cellular phenotype of the elevated cytosolic calcium levels due to Rnd3 deficiency. We found that the Rnd3 deficiency-induced abnormal calcium levels resulted in mitochondrial calcium overload and stress. The mitochondrial calcium overload disrupted normal oxidative phosphorylation, which led to elevated ROS generation and eventual cellular apoptosis. Inhibition of mitochondrial calcium uptake through Ru360 treatment attenuated mitochondrial calcium overload and stress, and partially rescued the Rnd3 deficiency-mediated mitochondrial dysfunction (Figure 7).

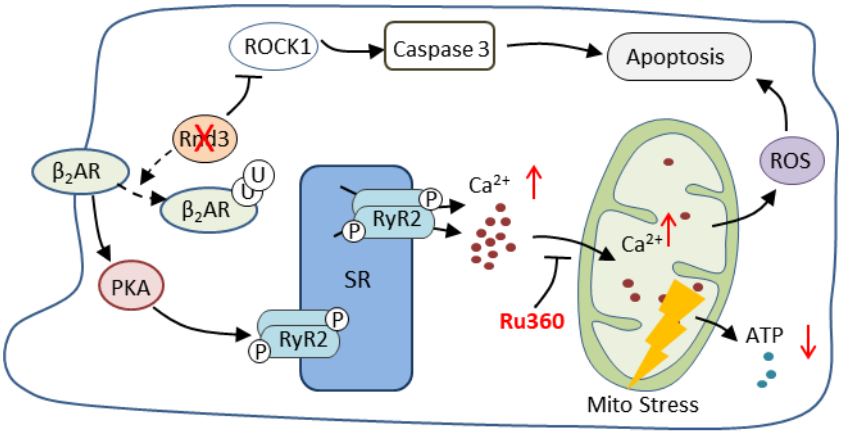

Figure 7. Mechanistic model for Rnd3 deficiency-mediated mitochondrial dysfunction and excessive ROS generation in cardiomyocytes. Rnd3 deficiency results in attenuation of β_2AR ubiquitination and degradation, which enhances PKA signaling. The excessive activation of PKA leads to hyperphosphorylation of RyR2, which in turn results in calcium leakage from the SR. The abnormal calcium stress causes mitochondrial calcium overload, disrupts normal oxidative phosphorylation, and leads to elevated ROS generation and eventual cellular apoptosis. Inhibition of the calcium uptake through Ru360 treatment attenuates mitochondrial calcium overload and stress, and partially rescues the Rnd3 deficiency-mediated mitochondrial dysfunction.
Abbreviations: SR: sarcoplasmic reticulum; U: ubiquitin; P: phosphorylation. β_2AR: β_2 adrenergic receptor; RyR2: ryanodine receptor 2; ROS: reactive oxygen species; ROCK1: Rho-associated coiled-coil protein kinase 1; PKA: protein kinase A.

4. CONCLUSION

Rnd3 deficiency results in elevated cytosolic calcium in cardiomyocytes through the accumulation of β_2AR and hyperactivation of the PKA signaling pathway; which ultimately results in destabilization of the SR RyR2 channels and calcium leakage [9]. Excessive cytosolic calcium is taken up by mitochondria and has massive effects on the mitochondrial membrane potential and overall function of the organelle.

The main function of myocardial mitochondria is to fulfill the high energy demands of the heart, which is critical for cardiomyocyte contraction. However, besides energy metabolism, mitochondria are involved in many biological processes including ROS generation, calcium homeostasis, and cellular apoptosis [20].The mitochondrial membrane potential ($\Delta\Psi m$) generated by oxidative phosphorylation via the electron transport chain is the energy source for ATP synthesis through the use of an electrochemical proton gradient across the inner mitochondrial membrane that drives ATP synthase. Disruption of the $\Delta\Psi m$ level is observed under pathological conditions such as hemodynamic stress, ischemia, and ischemia/reperfusion (I/R) injury; in which excessive ROS is generated due to a high $\Delta\Psi m$ level and is also associated with an increased intracellular calcium concentration [23, 24]. Both factors eventually promote the opening of the mitochondrial permeability transition pore (mPTP) and depolarization of the mitochondria, which lead to collapse of the $\Delta\Psi m$ and cytochrome c release. Consequently, ATP synthesis is further impaired and apoptosis is initiated. Many studies revealed that myocardial apoptosis along with caspase 3 activation was detected in end-stage heart failure patients [25-28]. Although the levels of apoptosis varied in the end-stage heart failure myocardial samples

[25, 29, 30], minimal levels of apoptosis were sufficient to cause cardiac contractile depression and contribute to the transition to heart failure [29, 31-37].

Our results showed hyperpolarized ΔΨm and impaired mitochondrial function in Rnd3$^{+/-}$ cardiomyocytes as a result of elevated calcium influx. Additionally, excessive ROS generation and apoptosis were detected in the mutant samples. Mitochondrial ROS is predominantly produced by complex I of the inner mitochondrial membrane electron transport chain in the form of superoxide ($O_2^{\bullet -}$). A significant increase in its production correlates to a lack of ATP production and a high NADH/NAD+ ratio in the mitochondrial matrix [38]. We showed uncoupled oxidative respiration as well as significantly decreased complex I driven ATP synthesis in mitochondria isolated from Rnd3$^{+/-}$ cardiomyocytes at the basal level and even more so after TAC or hypoxic stress. The Rnd3-deficiency mediated mitochondrial dysfunction was further demonstrated through excessive ROS detection in the mutant samples.

Physiological levels of ROS are important for redox signaling from the organelle to the rest of the cell. However, excessive levels can result in oxidative damage of mitochondrial proteins, membranes, and DNA; and can eventually lead to retrograde redox signaling. Mitochondrial outer membrane permeability (MOMP) is another consequence of mitochondrial oxidative damage, which promotes the release of intermembrane space proteins such as cytochrome c into the cytosol and initiates cellular apoptosis [38].

The entrance of calcium into the mitochondrial matrix requires the crossing of the outer mitochondrial membrane (OMM) and the inner mitochondrial membrane (IMM). While the detailed mechanisms of calcium influx/efflux regulation for the two membranes remain

unclear, the importance of voltage-dependent anion channels (VDACs) located on the OMM and mitochondrial calcium uniporter (MCU) on the IMM has been well documented [39, 40]. We conducted a series of experiments in WT and Rnd3$^{+/-}$ cardiomyocytes using Ru360, a well-known inhibitor of the VDACs and MCU [41]. We demonstrated that Ru360 treatment partially rescued the Rnd3-deficiency mediated mitochondrial dysfunction and excessive ROS generation under hypoxic conditions. Furthermore, Ru360 treatment significantly decreased the elevated level of apoptotic Rnd3$^{+/-}$ cardiomyocytes after hypoxia exposure.

Our data have uncovered a previously undisclosed function of Rnd3 in mitochondrial function and regulation, and provided a mechanistic consequence of Rnd3 downregulation as observed in heart failure patients [12]. The association amongst Rnd3 deficiency-mediated calcium dysregulation, mitochondrial stress, and cardiomyocyte apoptosis has been elucidated. Furthermore, the study has provided cellular evidence to support the concept that mitochondrial calcium overload contributes to heart failure [42]. The conclusion has provided a better understanding of the mechanism involved in many cardiomyopathies. We propose Rnd3 as a potential new target for pharmacological manipulations in the regulation of cytosolic as well as mitochondrial calcium and for the management of the detrimental effects of pathological calcium overload.

REFERENCES

[1] K. Riento, R.M. Guasch, R. Garg, B. Jin, A.J. Ridley, RhoE binds to ROCK I and inhibits downstream signaling, Mol Cell Biol 23(12) (2003) 4219-29.

[2] P.P. Ongusaha, H.G. Kim, S.A. Boswell, A.J. Ridley, C.J. Der, G.P. Dotto, Y.B. Kim, S.A. Aaronson, S.W. Lee, RhoE is a pro-survival p53 target gene that inhibits ROCK I-mediated apoptosis in response to genotoxic stress, Curr Biol 16(24) (2006) 2466-72.

[3] K. Wennerberg, M.A. Forget, S.M. Ellerbroek, W.T. Arthur, K. Burridge, J. Settleman, C.J. Der, S.H. Hansen, Rnd proteins function as RhoA antagonists by activating p190 RhoGAP, Curr Biol 13(13) (2003) 1106-15.

[4] K. Riento, P. Villalonga, R. Garg, A. Ridley, Function and regulation of RhoE, Biochem Soc Trans 33(Pt 4) (2005) 649-51.

[5] P. Chardin, Function and regulation of Rnd proteins, Nature reviews. Molecular cell biology 7(1) (2006) 54-62.

[6] R. Foster, K.Q. Hu, Y. Lu, K.M. Nolan, J. Thissen, J. Settleman, Identification of a novel human Rho protein with unusual properties: GTPase deficiency and in vivo farnesylation, Mol Cell Biol 16(6) (1996) 2689-99.

[7] X. Lin, B. Liu, X. Yang, X. Yue, L. Diao, J. Wang, J. Chang, Genetic deletion of Rnd3 results in aqueductal stenosis leading to hydrocephalus through up-regulation of Notch signaling, Proceedings of the National Academy of Sciences of the United States of America 110(20) (2013) 8236-41.

[8] X. Yue, X. Yang, X. Lin, T. Yang, X. Yi, Y. Dai, J. Guo, T. Li, J. Shi, L. Wei, G.C. Fan, C. Chen, J. Chang, Rnd3 haploinsufficient mice are predisposed to hemodynamic stress and develop apoptotic cardiomyopathy with heart failure, Cell Death Dis 5 (2014) e1284.

[9] X. Yang, T. Wang, X. Lin, X. Yue, Q. Wang, G. Wang, Q. Fu, X. Ai, D.Y. Chiang, C.Y. Miyake, X.H. Wehrens, J. Chang, Genetic Deletion of Rnd3/RhoE Results in Mouse Heart Calcium Leakage Through Upregulation of Protein Kinase A Signaling, Circ Res 116(1) (2015) e1-e10.

[10] P. Villalonga, R.M. Guasch, K. Riento, A.J. Ridley, RhoE inhibits cell cycle progression and Ras-induced transformation, Mol Cell Biol 24(18) (2004) 7829-40.

[11] E. Pacary, J. Heng, R. Azzarelli, P. Riou, D. Castro, M. Lebel-Potter, C. Parras, D.M. Bell, A.J. Ridley, M. Parsons, F. Guillemot, Proneural transcription factors regulate different steps of cortical neuron migration through Rnd-mediated inhibition of RhoA signaling, Neuron 69(6) (2011) 1069-84.

[12] X. Yue, X. Lin, T. Yang, X. Yang, X. Yi, X. Jiang, X. Li, T. Li, J. Guo, Y. Dai, J. Shi, L. Wei, K.A. Youker, G. Torre-Amione, Y. Yu, K.C. Andrade, J. Chang, Rnd3/RhoE Modulates Hypoxia-Inducible Factor 1alpha/Vascular Endothelial Growth Factor Signaling by Stabilizing Hypoxia-Inducible Factor 1alpha and Regulates Responsive Cardiac Angiogenesis, Hypertension 67(3) (2016) 597-605.

[13] B. Liu, X. Lin, X. Yang, H. Dong, X. Yue, K.C. Andrade, Z. Guo, J. Yang, L. Wu, X. Zhu, S. Zhang, D. Tian, J. Wang, Q. Cai, Q. Chen, S. Mao, Q. Chen, J. Chang, Downregulation of RND3/RhoE in glioblastoma patients promotes tumorigenesis through augmentation of notch transcriptional complex activity, Cancer Med 4(9) (2015) 1404-16.

[14] B. Liu, H. Dong, X. Lin, X. Yang, X. Yue, J. Yang, Y. Li, L. Wu, X. Zhu, S. Zhang, D. Tian, J. Wang, Q. Cai, S. Mao, Q. Chen, J. Chang, RND3 promotes Snail 1 protein degradation and inhibits glioblastoma cell migration and invasion, Oncotarget (2016).

[15] W. Jie, K.C. Andrade, X. Lin, X. Yang, X. Yue, J. Chang, Pathophysiological Functions of Rnd3/RhoE, Compr Physiol 6(1) (2015) 169-86.

[16] L. Paysan, L. Piquet, F. Saltel, V. Moreau, Rnd3 in Cancer: A Review of the Evidence for Tumor Promoter or Suppressor, Mol Cancer Res 14(11) (2016) 1033-1044.

[17] M. Vassalle, C.I. Lin, Calcium overload and cardiac function, J Biomed Sci 11(5) (2004) 542-65.

[18] C. Ozcan, M. Bienengraeber, D.M. Hodgson, D.L. Mann, A. Terzic, Mitochondrial tolerance to stress impaired in failing heart, J Mol Cell Cardiol 35(9) (2003) 1161-6.

[19] S. Javadov, C. Huang, L. Kirshenbaum, M. Karmazyn, NHE-1 inhibition improves impaired mitochondrial permeability transition and respiratory function during postinfarction remodelling in the rat, Journal of molecular and cellular cardiology 38(1) (2005) 135-43.

[20] H.E. Verdejo, A. del Campo, R. Troncoso, T. Gutierrez, B. Toro, C. Quiroga, Z. Pedrozo, J.P. Munoz, L. Garcia, P.F. Castro, S. Lavandero, Mitochondria, myocardial remodeling, and cardiovascular disease, Curr Hypertens Rep 14(6) (2012) 532-9.

[21] X. Lin, B. Liu, X. Yang, X. Yue, L. Diao, J. Wang, J. Chang, Genetic deletion of Rnd3 results in aqueductal stenosis leading to hydrocephalus through up-regulation of Notch signaling, Proceedings of the National Academy of Sciences of the United States of America (2013).

[22] C. Frezza, S. Cipolat, L. Scorrano, Organelle isolation: functional mitochondria from mouse liver, muscle and cultured fibroblasts, Nat Protoc 2(2) (2007) 287-95.

[23] B. Kadenbach, R. Ramzan, R. Moosdorf, S. Vogt, The role of mitochondrial membrane potential in ischemic heart failure, Mitochondrion 11(5) (2011) 700-6.

[24] M.N. Sack, Mitochondrial depolarization and the role of uncoupling proteins in ischemia tolerance, Cardiovasc Res 72(2) (2006) 210-9.

[25] J. Narula, N. Haider, R. Virmani, T.G. DiSalvo, F.D. Kolodgie, R.J. Hajjar, U. Schmidt, M.J. Semigran, G.W. Dec, B.A. Khaw, Apoptosis in myocytes in end-stage heart failure, N Engl J Med 335(16) (1996) 1182-9.

[26] J. Narula, P. Pandey, E. Arbustini, N. Haider, N. Narula, F.D. Kolodgie, B. Dal Bello, M.J. Semigran, A. Bielsa-Masdeu, G.W. Dec, S. Israels, M. Ballester, R. Virmani, S. Saxena, S. Kharbanda, Apoptosis in heart failure: release of cytochrome c from mitochondria and activation of caspase-3 in human cardiomyopathy, Proc Natl Acad Sci U S A 96(14) (1999) 8144-9.

[27] F. Blankenberg, J. Narula, H.W. Strauss, In vivo detection of apoptotic cell death: a necessary measurement for evaluating therapy for myocarditis, ischemia, and heart failure, J Nucl Cardiol 6(5) (1999) 531-9.

[28] A. Elsasser, K. Suzuki, J. Schaper, Unresolved issues regarding the role of apoptosis in the pathogenesis of ischemic injury and heart failure, J Mol Cell Cardiol 32(5) (2000) 711-24.

[29] G. Olivetti, R. Abbi, F. Quaini, J. Kajstura, W. Cheng, J.A. Nitahara, E. Quaini, C. Di Loreto, C.A. Beltrami, S. Krajewski, J.C. Reed, P. Anversa, Apoptosis in the failing human heart, N Engl J Med 336(16) (1997) 1131-41.

[30] J.C. Reed, G. Paternostro, Postmitochondrial regulation of apoptosis during heart failure, Proc Natl Acad Sci U S A 96(14) (1999) 7614-6.

[31] P.M. Kang, S. Izumo, Apoptosis and heart failure: A critical review of the literature, Circ Res 86(11) (2000) 1107-13.

[32] M.G. Yussman, T. Toyokawa, A. Odley, R.A. Lynch, G. Wu, M.C. Colbert, B.J. Aronow, J.N. Lorenz, G.W. Dorn, 2nd, Mitochondrial death protein Nix is induced in cardiac hypertrophy and triggers apoptotic cardiomyopathy, Nat Med 8(7) (2002) 725-30.

[33] B. Nadal-Ginard, J. Kajstura, P. Anversa, A. Leri, A matter of life and death: cardiac myocyte apoptosis and regeneration, J Clin Invest 111(10) (2003) 1457-9.

[34] D. Wencker, M. Chandra, K. Nguyen, W. Miao, S. Garantziotis, S.M. Factor, J. Shirani, R.C. Armstrong, R.N. Kitsis, A mechanistic role for cardiac myocyte apoptosis in heart failure, J Clin Invest 111(10) (2003) 1497-504.

[35] S. Yamamoto, G. Yang, D. Zablocki, J. Liu, C. Hong, S.J. Kim, S. Soler, M. Odashima, J. Thaisz, G. Yehia, C.A. Molina, A. Yatani, D.E. Vatner, S.F. Vatner, J. Sadoshima, Activation of Mst1 causes dilated cardiomyopathy by stimulating apoptosis without compensatory ventricular myocyte hypertrophy, J Clin Invest 111(10) (2003) 1463-74.

[36] J. Narula, E. Arbustini, Y. Chandrashekhar, M. Schwaiger, Apoptosis and the systolic dysfunction in congestive heart failure. Story of apoptosis interruptus and zombie myocytes, Cardiol Clin 19(1) (2001) 113-26.

[37] R.N. Kitsis, D.L. Mann, Apoptosis and the heart: a decade of progress, J Mol Cell Cardiol 38(1) (2005) 1-2.

[38] M.P. Murphy, How mitochondria produce reactive oxygen species, Biochem J 417(1) (2009) 1-13.

[39] R. Rizzuto, D. De Stefani, A. Raffaello, C. Mammucari, Mitochondria as sensors and regulators of calcium signalling, Nat Rev Mol Cell Biol 13(9) (2012) 566-78.

[40] T. Finkel, S. Menazza, K.M. Holmstrom, R.J. Parks, J. Liu, J. Sun, J. Liu, X. Pan, E. Murphy, The ins and outs of mitochondrial calcium, Circ Res 116(11) (2015) 1810-9.
[41] J. Garcia-Rivas Gde, K. Carvajal, F. Correa, C. Zazueta, Ru360, a specific mitochondrial calcium uptake inhibitor, improves cardiac post-ischaemic functional recovery in rats in vivo, Br J Pharmacol 149(7) (2006) 829-37.

[42] G. Santulli, W. Xie, S.R. Reiken, A.R. Marks, Mitochondrial calcium overload is a key determinant in heart failure, Proc Natl Acad Sci U S A 112(36) (2015) 11389-94.